

## Atlantic Meridional Overturning Circulation Decline: Tipping Small Scales under Global Warming

Ruijian Gou,<sup>1,2</sup> Gerrit Lohmann<sup>2,3,\*</sup> and Lixin Wu<sup>1,4</sup>

<sup>1</sup>*Frontiers Science Center for Deep Ocean Multispheres and Earth System and Key Laboratory of Physical Oceanography, Ocean University of China, Qingdao, China*

<sup>2</sup>*Alfred Wegener Institute, Helmholtz Centre for Polar and Marine Research, Bremerhaven, Germany*

<sup>3</sup>*University of Bremen, Bremen, Germany*

<sup>4</sup>*Laoshan Laboratory, Qingdao, China*

(Received 19 December 2023; accepted 10 June 2024)

The Atlantic circulation is a key component of the global ocean conveyor that transports heat and nutrients worldwide. Its likely weakening due to global warming has implications for climate and ecology. However, the expected changes remain largely uncertain as low-resolution climate models currently in use do not resolve small scales. Although the large-scale circulation tends to weaken uniformly in both the low-resolution and our high-resolution climate model version, we find that the small-scale circulation in the North Atlantic changes abruptly under global warming and exhibits pronounced spatial heterogeneity. Furthermore, the future Atlantic Ocean circulation in the high-resolution model version expands in conjunction with a sea ice retreat and strengthening toward the Arctic. Finally, the cutting-edge climate model indicates sensitive shifts in the eddies and circulation on regional scales for future warming and thus provides a benchmark for next-generation climate models that can get rid of parametrizations of unresolved scales.

DOI:

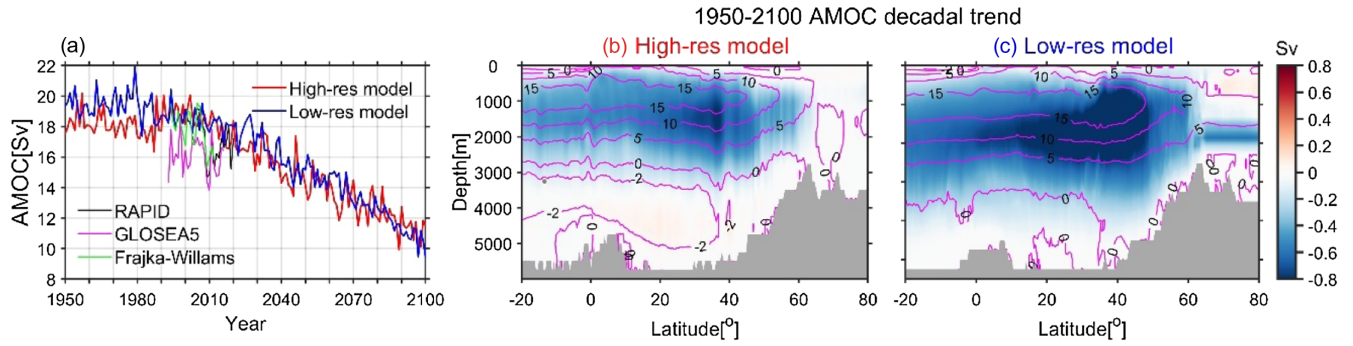
*Introduction.*—The Atlantic Meridional Overturning Circulation (AMOC), an important part of the global ocean conveyor, is projected to slow in the warming 21st century [1,2], as carbon dioxide emissions continue to increase and melting of the Greenland ice sheet accelerates [3]. Its decline would affect the Northern Hemisphere [4] and decelerate global carbon cycle [5]. Although a collapse of the large-scale AMOC (large scale means basin scale in this context) is unlikely in the near future [1,2], the regional scales are not investigated so far.

The small scales (in this context, ocean eddies and convection) are also crucial in climate and ecology. For example, the mesoscale eddies transport considerable heat [6] and nutrients [7]. Satellite observations have shown a global acceleration of eddy activity over the course of altimetry records [8]. Ocean convection, which forms deep water and transforms the upper limb of AMOC into lower limb, acts as heat [9] and carbon [10,11] pump. They have undergone some changes over the last decades [12–14]. Small-scale eddies play an important role in preconditioning and restratifying the water column before and after convection events, influencing the variability of deep water formation [15]. Simulations using high-resolution ocean and climate models, as well as measurements in key regions of the AMOC, indicate that the decline in AMOC over the past 20 years is primarily the result of weakened deep-water formation in the subarctic Atlantic [16]. Since the AMOC characterizes the zonally integrated circulation (Fig. 1), the

small scales might hold the key in understanding its changes [17–19].

However, projecting these small scales under future climate is challenging due to the low resolution of climate models [20]. The subarctic Atlantic, where convection and the overturning occur, is very rich in eddy activity. However, eddies are not resolved due to their small spatial scale. Simulation of convection is generally problematic, in part because it is modulated by misrepresented small-scale boundary currents and eddies [21]. In addition, the complex topography determines the dynamics of boundary currents and overflows. These small scales are not properly resolved in the current generation of climate models, so even AMOC predictions remain largely uncertain [17]. The projected AMOC collapse has a certain threshold [22,23], but the small scales could have different thresholds to collapse. The AMOC collapse is also suggested to be resolution dependent—the AMOC in higher-resolution model might be less sensitive to freshwater forcing and driven predominantly by internal feedbacks [22].

*Climate model.*—With the development of a high-resolution climate model [24], it is possible to assess how the AMOC and eddies may change [20]. Here, we use a cutting-edge high-resolution climate model [24] (herein-after abbreviated as HR), which has been used for studying small scales and corresponding regional climate and ecology in the other ocean basins [25–27] to examine AMOC and small scales in the subarctic Atlantic under



F1:1 FIG. 1. Atlantic Meridional Overturning Circulation under global warming. (a) Its annual-mean indices in HR (red line) and LR (blue  
 F1:2 line). The black, magenta, green lines, respectively, represent AMOC at 26°N observed by RAPID project (2005–2020) [30], a  
 F1:3 reconstruction from the GloSea5 reanalysis (1993–2016) [34], a reconstruction from satellite altimetry and cable measurements (1994–  
 F1:4 2012) [32]. (b),(c) Linear decadal trend over 1950–2100 in the stream function of HR (b) and LR (c). The solid magenta contours denote  
 F1:5 the long-term mean stream functions.

79 global warming. We also use a low-resolution analog  
 80 model version [24] to compare results (hereinafter abbrevi-  
 81 ated as LR).

82 The models used in this study are based on CESM1.3  
 83 [28]. HR has a nominal horizontal resolution of 0.1° in the  
 84 ocean and sea ice components and 0.25° in the atmosphere  
 85 and land components. LR has a nominal horizontal  
 86 resolution of 1°, which is consistent with most current  
 87 generation climate models [29]. The oceanic eddies are  
 88 parametrized in LR [30]. The time period of both versions  
 89 is 1950–2100, with 1950–2005 and 2006–2100, respec-  
 90 tively, applied with historical forcing and representative  
 91 concentration pathway 8.5 forcing (high CO<sub>2</sub> emission  
 92 scenario) [1,2]. The spin-up time is 250 years, with a  
 93 climate forcing fixed to preindustrial (year 1850) condi-  
 94 tions. The detailed setup of the models can be found in an  
 95 overview paper [24].

96 *Atlantic Meridional Overturning Circulation.*—The  
 97 AMOC stream function  $\Psi$  in the model [31] is defined as

$$\Psi(y, z) = \int_0^z \int_{x_w}^{x_e} v(x, y, \tilde{z}) dx d\tilde{z},$$

98 where  $x_e$  and  $x_w$  are the eastern and western boundaries of  
 100 the Atlantic basin,  $v$  is the meridional velocity. The AMOC  
 101 index is defined as the spatial maximum of  $\Psi$  at 26°N.

102 The AMOC indices are surprisingly consistent between  
 103 HR and LR [Fig. 1(a)]. Their magnitude is comparable to  
 104 the observation [32] and reconstructions [33,34] of AMOC  
 105 at 26°N. The AMOC indices in both models similarly  
 106 decline by  $\sim 8$  Sv from 2000 to 2100 CE with the sharpest  
 107 decline beginning in  $\sim 2020$ . The AMOC decline reflected  
 108 in the spatial distributions of the trends is somewhat weaker  
 109 in HR [Figs. 1(b) and 1(c)]. It is suggested to be modulated  
 110 by the resolved processes in HR: the better resolved  
 111 Labrador Current limits the offshore transport of freshwater  
 112 from Arctic Ocean into the convection region, and thereby  
 113 the decline in Labrador Sea overturning is weaker in

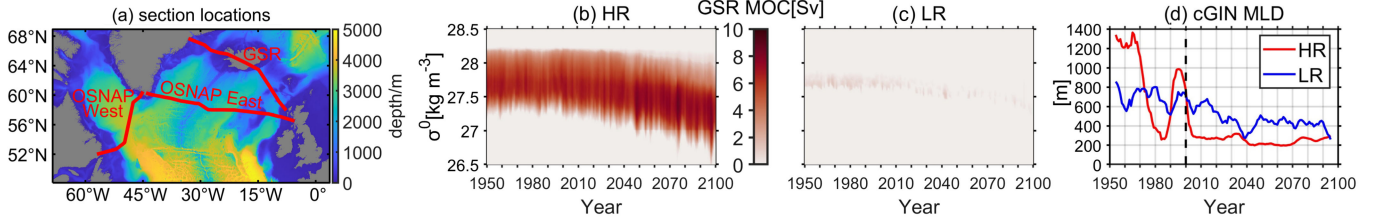
HR [35]. The mean states of AMOC show larger  
 114 differences [Figs. 1(b) and 1(c) magenta lines]. In HR,  
 115 the upper limb of North Atlantic deep water is shallower.  
 116 This is attributed to the no longer necessary parametrization  
 117 for the Nordic Sea overflows and stronger Antarctica  
 118 Bottom Water flow in HR [24]. Although the large-scale  
 119 AMOC indices are very similar between the model  
 120 versions, the changes in the spatial structure of AMOC  
 121 are more evident in the high-resolution model. The AMOC  
 122 indices cannot reflect regional-scale changes either  
 123 [31,36,37], which is detected in other basins of HR [25,27].  
 124

The overturning stream function across sections (MOC <sub>$\sigma$</sub> )  
 125 is defined as [38]  
 126

$$\text{MOC}_\sigma(\sigma, t) = \int_{\sigma_{\min}}^{\sigma} d\sigma \int_{s_w}^{s_e} v(s, \sigma, t) ds,$$

127 where  $s_w$  and  $s_e$  are the western and eastern boundaries of  
 128 the sections,  $s$  is the distance coordinate along the sections,  
 129  $v$  is the velocity perpendicular to the sections,  $\sigma$  is the  
 130 potential density referenced to 0 m. The integral of density  
 131 is taken from the surface density ( $\sigma_{\min}$ ) across all density  
 132 surfaces. The maximum of MOC <sub>$\sigma$</sub>  at a certain time is  
 133 recognized as the magnitude of AMOC at the sections.  
 134

135 The Subpolar North Atlantic Program (OSNAP) sections  
 136 [Fig. 2(a)] are designed to observe the western and eastern  
 137 overturning in the subarctic Atlantic since 2014 [38]. In  
 138 HR, the overturning in the subarctic Atlantic compares  
 139 better with the observations, in terms of magnitude and  
 140 variability (Fig. 2 in [39], Fig. S1). The detailed analysis is  
 141 provided in Supplemental Material [40] (see also  
 142 Refs. [41–54] therein). Further north at the Greenland-  
 143 Scotland Ridge [GSR; Fig. 2(a)], an overflow parametriza-  
 144 tion is not used for HR, in contrast to LR. Here, we see an  
 145 increase of AMOC in HR [Fig. 2(b)], which is the opposite  
 146 to the decline at 26°N and OSNAP sections. While in LR,  
 147 there is almost no overturning and also no increase  
 148 [Fig. 2(c)].



F2:1 FIG. 2. Meridional Overturning Circulation in the North Atlantic. (a) The locations of the three sections—OSNAP West, OSNAP East,  
 F2:2 and Greenland-Scotland Ridge (GSR). Color shading denotes the ocean depth. (b),(c) Hovmöller diagram of  $MOC_{\sigma}$  at GSR during  
 F2:3 1950–2100 in HR (b) and LR (c). (d) Area-mean March mixed layer depth in the Nordic Sea (averaging areas are shown in Fig. S3 [40]),  
 F2:4 smoothed by a 10-year running mean. The vertical dashed line denotes a tipping point.

149 This amplification of AMOC suggests that ventilation  
 150 and subduction north of the GSR is increasing under global  
 151 warming. As sea ice retreats and open-ocean area increases,  
 152 air-sea interaction enhances ocean mixing. This leads to an  
 153 strengthening of AMOC toward the Arctic, as projected by  
 154 climate modeling [48] that indicates sites of convection and  
 155 subduction moving northward to the central Arctic with  
 156 global warming. Reference [55] also found AMOC  
 157 emerges beyond the GSR, which strengthens as the areas  
 158 of deep mixing move northward toward the central Arctic  
 159 following sea ice retreat. In addition, there is observational  
 160 evidence supporting increased mixing and convection as  
 161 the sea ice edge retreats [56,57]. Our results in HR support  
 162 the hypothesis that the AMOC intensifies toward the Arctic  
 163 under global warming.

164 Following the decline in sea ice, several locations show  
 165 weakly increasing trends of march mixed layer depth  
 166 (MLD, representing the convection strength [48], definition  
 167 written in Supplemental Material) (Fig. S3d [40]). The  
 168 convection in the Nordic Sea shows a tipping point at the  
 169 year 2000 for both models [Fig. 2(d)]. In HR, the MLD  
 170 strongly declines to a minimum of  $\sim 300$  m in the 1980s,  
 171 and then rising abruptly to 1000 m in 1990s. A similar  
 172 decline was observed in the 1980s [58] and recovery in the  
 173 1990s [59]. After 2000, it drops to  $\sim 200$  m and then  
 174 remains stable, indicating that convection has almost  
 175 collapsed. In LR, the MLD begins to decline in 2000  
 176 and remains  $\sim 400$  m since 2020 CE. The variability in HR  
 177 is more abrupt and step-wise. Regarding the convection in  
 178 the other seas, one can refer to Supplemental Material [40].  
 179 To summarize, at the regional scale in the North Atlantic,  
 180 HR outperforms LR in simulating local circulations and  
 181 shows a completely different response of the AMOC to  
 182 global warming. When representing regional ocean circulations,  
 183 the small scales should be key.

184 *Eddy kinetic energy.*—The eddy kinetic energy (EKE)  
 185 reflects the strength of eddy activity in the ocean. The eddy  
 186 activity is not resolved and parametrized in LR [30]. The  
 187 detailed discussion of regional EKE changes in HR is  
 188 written in Supplemental Material [40]. The EKE is calcu-  
 189 lated based on sea surface height from HR, which will be  
 190 referred as  $\eta$  hereinafter. First, the daily surface geostrophic  
 191 velocity  $(u_g, v_g)$  is calculated as

$$u_g = \frac{-g}{f} \frac{\partial \eta}{\partial x}, \quad v_g = \frac{g}{f} \frac{\partial \eta}{\partial y},$$

193 where the gravitational acceleration  $g = 9.81 \text{ m s}^{-2}$ ,  
 194 Coriolis frequency  $f = 2\Omega \sin \varphi$  with the angular speed  
 195 of Earth  $\Omega = 7.292 \times 10^{-5} \text{ rad s}^{-1}$  and latitude  $\varphi$ .  
 196 Afterward the perturbation  $(u'_g, v'_g)$  is defined as

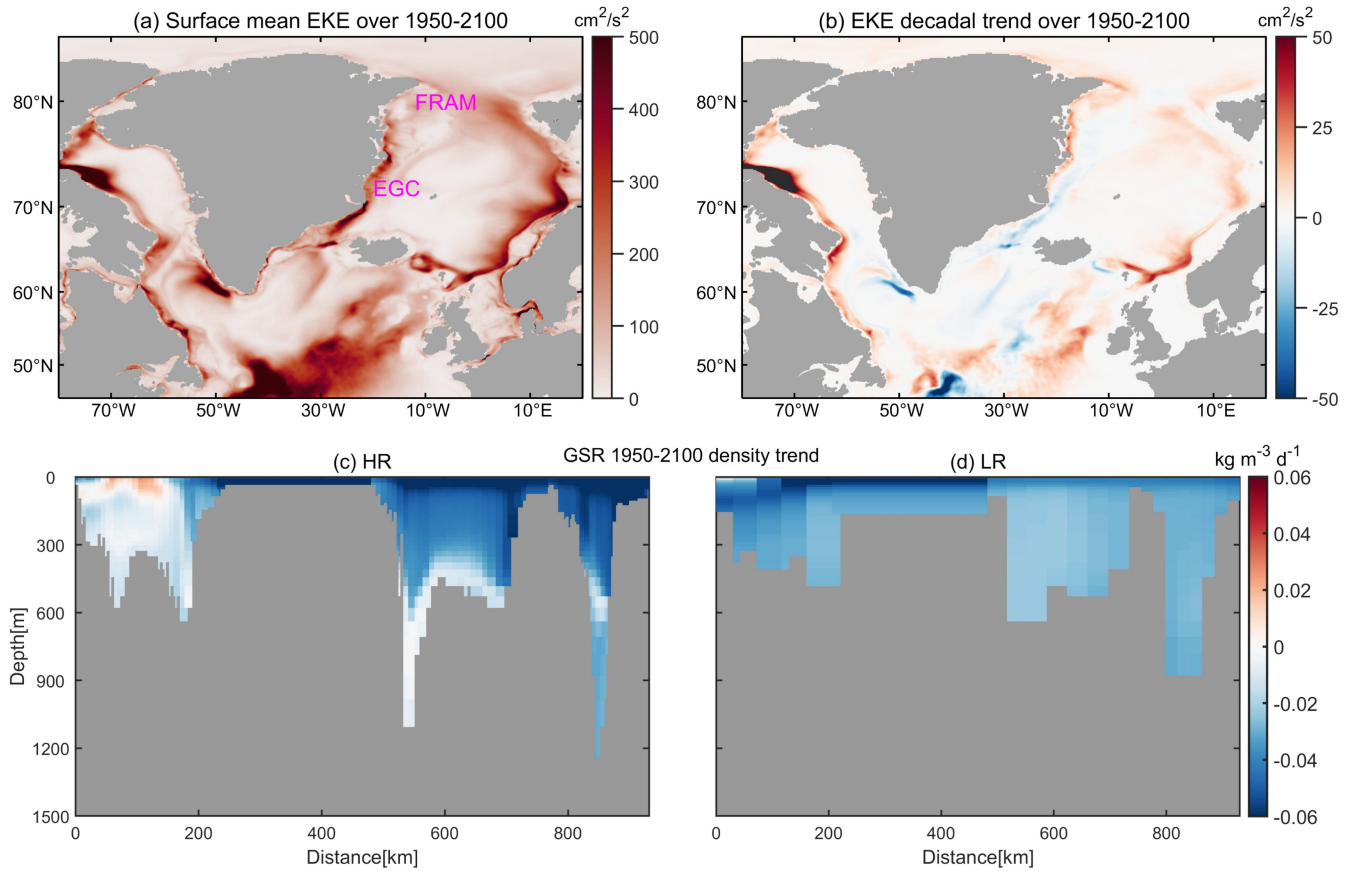
$$u'_g = u_g - \overline{u_g}, \quad v'_g = v_g - \overline{v_g},$$

198 where the overbar denotes annual mean.  $(u'_g, v'_g)$  does not  
 199 contain interannual variability and is recognized as eddy  
 200 velocity [60]. Therefore, the EKE is calculated as **Q1**

$$\text{EKE} = \frac{1}{2} (u_g'^2 + v_g'^2).$$

203 Prominent shifts in the eddy activity, which are key to  
 204 regional climate change, occur under the background of a  
 205 moderately declining AMOC [Fig. 3(b) and Fig. S2 [40]].  
 206 The enhanced EKE near Fram Strait is related to the  
 207 increasing freshwater outflow (due to sea ice retreat) that  
 208 increases barotropic instability, as well as the increasing  
 209 freshwater presence inshore that increases the horizontal  
 210 density gradient and thus baroclinic instability. The eddy  
 211 activity causes freshwater spread into the convection region  
 212 in the GIN sea and thus its variability could be partly related  
 213 to the HR shifts in the convection. Given the lateral  
 214 freshwater spread, the EKE decrease as seen in the  
 215 following EGC could be due to a decreased velocity and **Q2**  
 216 density gradient. This further leads to a stable (and even  
 217 increasing) density in the EGC [Fig. 3(c)] in HR. While in  
 218 LR, the density decrease across the GSR section is  
 219 generally uniform [Fig. 3(d)]. In HR, the contrast in the  
 220 west-east density change [Fig. 3(c)] causes a regional  
 221 AMOC increase at the GSR section.

222 *Discussion.*—Eddies are ubiquitous in the world ocean  
 223 and alter seawater properties, ocean circulation, biogeo-  
 224 chemical fluxes, and mixed-layer properties [61]. In the  
 225 North Atlantic, GIN Sea and Barents Sea, pronounced  
 226 mixed layer anomalies and very energetic mesoscale eddies  
 227 are observed [62], suggesting a robust relationship between  
 228 eddy amplitude and mixed layer variations [15]. In



F3:1 FIG. 3. Surface eddy kinetic energy and density distribution in the subarctic Atlantic under global warming. (a),(b) Mean (a) and linear  
 F3:2 decadal trend (b) of EKE over 1950–2100 in HR. FRAM and EGC, respectively represent East Greenland Current and Fram Strait. (c),  
 F3:3 (d) Linear decadal trend over 1950–2100 of density at the GSR section in HR (c) and LR (d).

229 addition, eddies near deep convection and boundary cur- 252  
 230 rents cause flattening of steep isopycnals [63], affecting 253  
 231 directly deep-water formation and thus AMOC. Given the 254  
 232 slowing of AMOC and the potential crossing of a tipping 255  
 233 point in the future [64], our study suggests that the feedback 256  
 234 between AMOC and small scales could change in the 257  
 235 future. High-resolution climate modeling provides new 258  
 236 opportunities to study the links between eddies, convection, 259  
 237 and AMOC under climate change. 260

238 Although the decrease in the AMOC index under global 261  
 239 warming is basically the same in HR and LR, HR changes 262  
 240 the AMOC structure and eddy activity significantly. In HR, 263  
 241 abrupt shifts in regional circulation and eddy activity are 264  
 242 detected under global warming: the AMOC shows a 265  
 243 strengthening trend at GSR, suggesting enhanced ventila- 266  
 244 tion toward the Arctic, which is only seen in HR. 267  
 245 Convection nearly ceases after 2000 CE in the eastern 268  
 246 subpolar gyre, in contrast to a moderately decreasing 269  
 247 convection in LR. The change in eddy activity indicates 270  
 248 significant spatial heterogeneity: substantial increase 271  
 249 around Fram Strait and decrease in the EGC induce the 272  
 250 AMOC increase at GSR by altering the density distribution. 273  
 251 To summarize, it is likely that the small and regional scales 274

of AMOC have different tipping points compared to the 252  
 general AMOC. 253

254 Consequently, the upper-ocean variability and water 255  
 256 mass properties can strongly differ between high and 257  
 258 low resolution [65]. The shifts in the eddy activity imply 259  
 260 an abrupt change in the pattern of horizontal movement of 261  
 262 heat and nutrients under global warming. The resulting 263  
 264 convection shifts imply the transition in the vertical move- 265  
 266 ment of heat and nutrients. Although the AMOC is 267  
 268 uniformly decreasing, the regional redistribution of heat 269  
 270 and nutrients may be transitioning to a different state 271  
 272 because of the small-scale shifts. This can be crucial when 273  
 274 we try to reconstruct large-scale AMOC shifts that have 275  
 occurred in the past, based on limited spatial informa- 276  
 tion [66]. 277

278 We conclude that the interplay between convection, eddy 279  
 280 activity, and AMOC is scale dependent, posing a challenge 281  
 282 for the large-scale circulation and mesoscale features in a 283  
 284 warming ocean. In the 1970s, the framework for climate 285  
 286 models was established [67,68], and a prototype climate 287  
 288 model was used to demonstrate that anthropogenic  $\text{CO}_2$  is 289  
 290 causing global warming [69]. Since then, given the limita- 291  
 292 tion of model resolution, the focus of research has been 293  
 294

275 on large-scale climate pattern that are externally driven.  
 276 With the developing computing capacities, it is time to  
 277 “think big and model small” [18], to understand the meso-  
 278 scale changes which can hold a key for surprises [70].  
 279 Regional high-resolution climate models like Med-  
 280 CORDEX aiming at Mediterranean climate [71] have  
 281 shown series of impacts from model resolution and  
 282 resolved processes on regional climate. Incorporating the  
 283 interplay of small-scale processes is key to assess the large-  
 284 scale ocean evolution, but also requires direct observations  
 285 at critical locations. On the other hand, the observed decline  
 286 in AMOC at 26 °N over the past two decades [72,73] is now  
 287 placed in the context of actual small-scale shifts that cannot  
 288 be simply inferred from the AMOC decline at a certain  
 289 latitude.

290  
 291 The data that support the findings of this study are  
 292 available upon request.

293 Q3 R. G. received support from the exchange program  
 294 (57606984) of the German Academic Exchange Service  
 295 (DAAD) and the Fundamental Research Funds for the  
 296 Central Universities. G. L. acknowledges financial support  
 297 by PACES and REKLIM through the Alfred Wegener  
 298 Institute in the Helmholtz association, as well as from  
 299 PalMod and ACE projects through the German Federal  
 300 Ministry of Education and Research. Development of the  
 301 CESM 1.3 model and computational resources were made  
 302 available by National Center for Atmospheric Research  
 303 (NCAR), Qingdao Pilot National Laboratory for Marine  
 304 Science and Technology (QNLN), and Texas A&M  
 305 University (TAMU). We thank Laura C. Jackson and  
 306 Eleanor Frajka-Williams for providing the reconstructed  
 307 AMOC data, Stephen Yeager for providing the codes  
 308 in calculating the AMOC across OSNAP sections,  
 309 Paul G. Myers from University of Alberta for a discussion  
 310 on the data analysis, Ke Xiao and Yitian Huang for making  
 311 Q4 one of the plots.

312 R. G. performed the analysis, G. L. proposed the central  
 313 idea, R. G. and G. L. wrote the paper, L. W. conceived the  
 314 project, and all authors contributed to improving the  
 315 manuscript.

316  
 317 The authors declare no competing financial interests.

318  
 319 \*Contact author: Gerrit.Lohmann@awi.de

320 [1] V. Masson-Delmotte, P. Zhai, A. Pirani, S. L. Connors, C.  
 321 Péan, S. Berger, N. Caud, Y. Chen, L. Goldfarb, M. Gomis  
 322 *et al.*, Climate change 2021: The physical science basis,  
 323 *Contribution of Working Group I to the Sixth Assessment*  
 324 *Report of the Intergovernmental Panel on Climate Change*  
 325 Q5 (2021), Vol. 2.  
 326

- [2] H.-O. Pörtner, D. C. Roberts, V. Masson-Delmotte, P. Zhai, 327  
 M. Tignor, E. Poloczanska, and N. Weyer, The ocean and 328  
 cryosphere in a changing climate, *IPCC Special Report on 329*  
*the Ocean and Cryosphere in a Changing Climate* (2019), 330  
 Vol. 1155. 331
- [3] L. Ackermann, C. Danek, P. Gierz, and G. Lohmann, 332  
 AMOC recovery in a multicentennial scenario using a 333  
 coupled atmosphere-ocean-ice sheet model, *Geophys. 334*  
*Res. Lett.* **47**, e2019GL086810 (2020). 335
- [4] L. Jackson, R. Kahana, T. Graham, M. Ringer, T. Woollings, 336  
 J. Mecking, and R. Wood, Global and European climate 337  
 impacts of a slowdown of the AMOC in a high resolution 338  
 GCM, *Clim. Dyn.* **45**, 3299 (2015). 339
- [5] K. Zickfeld, M. Eby, and A. J. Weaver, Carbon-cycle 340  
 feedbacks of changes in the Atlantic meridional overturning 341  
 circulation under future atmospheric CO<sub>2</sub>, *Global Biogeo- 342*  
*chem Cycles* **22** (2008). 343
- [6] Z. Zhang, W. Wang, and B. Qiu, Oceanic mass transport by 344  
 mesoscale eddies, *Science* **345**, 322 (2014). 345
- [7] D. B. Chelton, P. Gaube, M. G. Schlax, J. J. Early, and R. M. 346  
 Samelson, The influence of nonlinear mesoscale eddies 347  
 on near-surface oceanic chlorophyll, *Science* **334**, 328 348  
 (2011). 349
- [8] J. Martínez-Moreno, A. M. Hogg, M. H. England, N. C. 350  
 Constantinou, A. E. Kiss, and A. K. Morrison, Global 351  
 changes in oceanic mesoscale currents over the satellite 352  
 altimetry record, *Nat. Clim. Change* **11**, 397 (2021). 353
- [9] J. M. Gregory, Vertical heat transports in the ocean and their 354  
 effect on time-dependent climate change, *Clim. Dyn.* **16**, 355  
 501 (2000). 356
- [10] F. Frob, A. Olsen, K. Vage, G. Moore, I. Yashayaev, E. 357  
 Jeansson, and B. Rajasakaren, Irminger sea deep convection 358  
 injects oxygen and anthropogenic carbon to the ocean 359  
 interior, *Nat. Commun.* **7**, 13244 (2016). 360
- [11] M. Rhein, R. Steinfeldt, D. Kieke, I. Stendardo, and I. 361  
 Yashayaev, Ventilation variability of Labrador Sea water and 362  
 its impact on oxygen and anthropogenic carbon: A review, 363  
*Phil. Trans. R. Soc. A* **375** (2017). 364
- [12] K. Våge, R. S. Pickart, V. Thierry, G. Reverdin, C. M. Lee, 365  
 B. Petrie, T. A. Agnew, A. Wong, and M. H. Ribergaard, 366  
 Surprising return of deep convection to the subpolar North 367  
 Atlantic Ocean in winter 2007–2008, *Nat. Geosci.* **2**, 67 368  
 (2009). 369
- [13] G. W. K. Moore, K. Våge, R. S. Pickart, and I. A. Renfrew, 370  
 Decreasing intensity of open-ocean convection in the Green- 371  
 land and Iceland seas, *Nat. Clim. Change* **5**, 877 (2015). 372
- [14] I. Yashayaev and J. W. Loder, Further intensification of deep 373  
 convection in the Labrador Sea in 2016, *Geophys. Res. Lett.* 374  
**44**, 1429 (2017). 375
- [15] C. Danek, P. Scholz, and G. Lohmann, Decadal variability 376  
 of eddy temperature fluxes in the Labrador Sea, *Ocean 377*  
*Modelling* **182** (2023). 378
- [16] L. C. Jackson, A. Biastoch, M. W. Buckley, D. G. 379  
 Desbruyères, E. Frajka-Williams, B. Moat, and J. 380  
 Robson, The evolution of the North Atlantic Meridional 381  
 Overturning Circulation since 1980, *Nat. Rev. Earth Envi- 382*  
*ron.* **3**, 241 (2022). 383
- [17] H. Hewitt, B. Fox-Kemper, B. Pearson, M. Roberts, and D. 384  
 Klocke, The small scales of the ocean may hold the key to 385  
 surprises, *Nat. Clim. Change* **12**, 496 (2022). 386

- 387 [18] Think big and model small, *Nat. Clim. Change* **12**, 493  
 388 **Q7** (2022). 447
- 389 [19] J. Marshall, J. R. Scott, A. Romanou, M. Kelley, and A.  
 390 Leboissetier, The dependence of the ocean's MOC on  
 391 mesoscale eddy diffusivities: A model study, *Ocean Mod-*  
 392 *elling* **111**, 1 (2017). 448
- 393 [20] S. Rahmstorf, Shifting seas in the greenhouse?, *Nature*  
 394 (London) **399**, 523 (1999). 449
- 395 [21] J. Marshall and F. Schott, Open-ocean convection: Obser-  
 396 vations, theory, and models, *Rev. Geophys.* **37**, 1 (1999). 450
- 397 [22] P. Ditlevsen and S. Ditlevsen, Warning of a forthcoming  
 398 collapse of the Atlantic Meridional Overturning Circulation,  
 399 *Nat. Commun.* **14**, 4254 (2023). 451
- 400 [23] R. M. van Westen, M. Kliphuis, and H. A. Dijkstra, Physics-  
 401 based early warning signal shows that AMOC is on tipping  
 402 course, *Sci. Adv.* **10**, eadk1189 (2024). 452
- 403 [24] P. Chang, S. Zhang, G. Danabasoglu, S. G. Yeager, H. Fu,  
 404 H. Wang, F. S. Castruccio, Y. Chen, J. Edwards, D. Fu *et al.*,  
 405 An unprecedented set of high-resolution Earth system  
 406 simulations for understanding multiscale interactions in  
 407 climate variability and change, *J. Adv. Model. Earth Syst.*  
 408 **12** (2020). 453
- 409 [25] Z. Jing, S. Wang, L. Wu, P. Chang, Q. Zhang, B. Sun, X.  
 410 Ma, B. Qiu, J. Small, F.-F. Jin *et al.*, Maintenance of mid-  
 411 latitude oceanic fronts by mesoscale eddies, *Sci. Adv.* **6**  
 412 **Q8** (2020). 454
- 413 [26] X. Guo, Y. Gao, S. Zhang, L. Wu, P. Chang, W. Cai, J.  
 414 Zscheischler, L. R. Leung, J. Small, G. Danabasoglu *et al.*,  
 415 Threat by marine heatwaves to adaptive large marine  
 416 ecosystems in an eddy-resolving model, *Nat. Clim. Change*  
 417 **12**, 179 (2022). 455
- 418 [27] S. Wang, Z. Jing, L. Wu, W. Cai, P. Chang, H. Wang, T.  
 419 Geng, G. Danabasoglu, Z. Chen, X. Ma *et al.*, El Niño/  
 420 Southern Oscillation inhibited by submesoscale ocean  
 421 eddies, *Nat. Geosci.* **15**, 112 (2022). 456
- 422 [28] S. Zhang, H. Fu, L. Wu, Y. Li, H. Wang, Y. Zeng, X. Duan,  
 423 W. Wan, L. Wang, Y. Zhuang *et al.*, Optimizing high-  
 424 resolution community Earth system model on a hetero-  
 425 geneous many-core supercomputing platform, *Geosci.*  
 426 *Model Dev.* **13**, 4809 (2020). 457
- 427 [29] V. Eyring, S. Bony, G. A. Meehl, C. A. Senior, B. Stevens,  
 428 R. J. Stouffer, and K. E. Taylor, Overview of the coupled  
 429 model intercomparison project phase 6 (CMIP6) experi-  
 430 mental design and organization, *Geosci. Model Dev.* **9**, 1937  
 431 (2016). 458
- 432 [30] P. R. Gent, J. Willebrand, T. J. McDougall, and J. C.  
 433 McWilliams, Parameterizing eddy-induced tracer transports  
 434 in ocean circulation models, *J. Phys. Oceanogr.* **25**, 463  
 435 (1995). 459
- 436 [31] M. J. Roberts, L. C. Jackson, C. D. Roberts, V. Meccia, D.  
 437 Docquier, T. Koenigk, P. Ortega, E. Moreno-Chamarro, A.  
 438 Bellucci, A. Coward *et al.*, Sensitivity of the Atlantic  
 439 Meridional Overturning Circulation to model resolution  
 440 in CMIP6 HighResMIP simulations and implications for  
 441 future changes, *J. Adv. Model. Earth Syst.* **12**,  
 442 **Q9** e2019 MS002014 (2020). 460
- 443 [32] J. Robson, D. Hodson, E. Hawkins, and R. Sutton, Atlantic  
 444 overturning in decline?, *Nat. Geosci.* **7**, 2 (2014). 461
- 445 [33] L. C. Jackson, K. A. Peterson, C. D. Roberts, and R. A.  
 446 Wood, Recent slowing of Atlantic overturning circulation as  
 a recovery from earlier strengthening, *Nat. Geosci.* **9**, 518  
 (2016). 462
- [34] E. Frajka-Williams, Estimating the Atlantic overturning at  
 26°N using satellite altimetry and cable measurements,  
*Geophys. Res. Lett.* **42**, 3458 (2015). 463
- [35] X. Shan, S. Sun, L. Wu, and M. Spall, Roles of the Labrador  
 current in the Atlantic meridional overturning circulation  
 responses to greenhouse warming (2024). **Q10** 464
- [36] S. Rahmstorf, J. E. Box, G. Feulner, M. E. Mann, A.  
 Robinson, S. Rutherford, and E. J. Schaffernicht,  
 Exceptional twentieth-century slowdown in Atlantic Ocean  
 overturning circulation, *Nat. Clim. Change* **5**, 475  
 (2015). 465
- [37] W. Weijer, W. Cheng, O. A. Garuba, A. Hu, and B. Nadiga,  
 CMIP6 models predict significant 21st century decline of  
 the Atlantic Meridional Overturning Circulation, *Geophys.*  
*Res. Lett.* **47** (2020). 466
- [38] M. S. Lozier, F. Li, S. Bacon, F. Bahr, A. S. Bower, S.  
 Cunningham, M. F. de Jong, L. de Steur, B. deYoung, J.  
 Fischer *et al.*, A sea change in our view of overturning in the  
 subpolar North Atlantic, *Science* **363**, 516 (2019). 467
- [39] S. Yeager, F. Castruccio, P. Chang, G. Danabasoglu, E.  
 Maroon, J. Small, H. Wang, L. Wu, and S. Zhang, An  
 outsized role for the Labrador Sea in the multidecadal  
 variability of the Atlantic overturning circulation, *Sci. Adv.*  
**7** (2021). **Q11** 472
- [40] See Supplemental Material at <http://link.aps.org/supplemental/10.1103/PhysRevLett.000.000000> for addi-  
 tional information about the model results and validations,  
 which includes Refs. [41–54]. 473
- [41] M. S. Lozier, Overturning in the North Atlantic, *Annu. Rev.*  
*Mar. Sci.* **4**, 291 (2012). 474
- [42] M. B. Menary, L. C. Jackson, and M. S. Lozier, Reconciling  
 the relationship between the AMOC and Labrador Sea in  
 OSNAP observations and climate models, *Geophys. Res.*  
*Lett.* **47**, e2020GL089793 (2020). 475
- [43] S. Zou, M. S. Lozier, F. Li, R. Abernathy, and L. Jackson,  
 Density-compensated overturning in the Labrador Sea, *Nat.*  
*Geosci.* **13**, 121 (2020). 476
- [44] J. M. Lilly, P. B. Rhines, F. Schott, K. Lavender, J. Lazier, U.  
 Send, and E. D'Asaro, Observations of the Labrador Sea  
 eddy field, *Progr. Oceanogr.* **59**, 75 (2003). 477
- [45] O. Johannessen, J. Johannessen, E. Svendsen, R.  
 Shuchman, W. Campbell, and E. Josberger, Ice-edge eddies  
 in the Fram Strait marginal ice zone, *Science* **236**, 427  
 (1987). 478
- [46] G. Lohmann and R. Gerdes, Sea ice effects on the sensitivity  
 of the thermohaline circulation in simplified atmosphere-  
 ocean-sea ice models, *J. Clim.* **11**, 2789 (1998). 479
- [47] T. Hattermann, P. E. Isachsen, W.-J. von Appen, J.  
 Albretsen, and A. Sundfjord, Eddy-driven recirculation of  
 Atlantic water in Fram Strait, *Geophys. Res. Lett.* **43**, 3406  
 (2016). 480
- [48] C. Lique and M. D. Thomas, Latitudinal shift of the  
 Atlantic Meridional Overturning Circulation source regions  
 under a warming climate, *Nat. Clim. Change* **8**, 1013  
 (2018). 481
- [49] F. Tagklis, A. Bracco, T. Ito, and R. Castelao, Submesoscale  
 modulation of deep water formation in the Labrador Sea,  
*Sci. Rep.* **10**, 17489 (2020). 482

- 507 [50] L. Caesar, S. Rahmstorf, A. Robinson, G. Feulner, and V. Saba, Observed fingerprint of a weakening Atlantic Ocean overturning circulation, *Nature (London)* **556**, 191 (2018). 548
- 508 549
- 509 550
- 510 [51] B. Qiu, T. Nakano, S. Chen, and P. Klein, Submesoscale transition from geostrophic flows to internal waves in the northwestern Pacific upper ocean, *Nat. Commun.* **8**, 14055 (2017). 551
- 511 552
- 512 553
- 513 554
- 514 [52] C. Deser, M. Holland, G. Reverdin, and M. Timlin, Decadal variations in Labrador Sea ice cover and North Atlantic sea surface temperatures, *J. Geophys. Res.* **107**, 3 (2002). 555
- 515 556
- 516 [53] S. Jónsson, A. Foldvik, and K. Aagaard, The structure and atmospheric forcing of the mesoscale velocity field in Fram Strait, *J. Geophys. Res.* **97**, 12585 (1992). 557
- 517 558
- 518 559
- 519 560
- 520 [54] W.-J. von Appen, T. M. Baumann, M. Janout, N. Koldunov, Y.-D. Lenn, R. S. Pickart, R. B. Scott, and Q. Wang, Eddies and the distribution of eddy kinetic energy in the Arctic Ocean, *Oceanography* **35**, 42 (2022). 561
- 521 562
- 522 563
- 523 564
- 524 [55] A. Bretones, K. H. Nisancioglu, M. F. Jensen, A. Brakstad, and S. Yang, Transient increase in arctic deep-water formation and ocean circulation under sea ice retreat, *J. Clim.* **35**, 109 (2022). 565
- 525 566
- 526 567
- 527 568
- 528 [56] K. Våge, L. Papritz, L. Håvik, M. A. Spall, and G. W. K. Moore, Ocean convection linked to the recent ice edge retreat along east Greenland, *Nat. Commun.* **9**, 1 (2018). 569
- 529 570
- 530 571
- 531 [57] G. W. K. Moore, K. Våge, I. A. Renfrew, and R. S. Pickart, Sea-ice retreat suggests re-organization of water mass transformation in the Nordic and Barents Seas, *Nat. Commun.* **13**, 1 (2022). 572
- 532 573
- 533 574
- 534 575
- 535 [58] P. Schlosser, G. Bönisch, M. Rhein, and R. Bayer, Reduction of deepwater formation in the Greenland Sea during the 1980s: Evidence from tracer data, *Science* **251**, 1054 (1991). 576
- 536 577
- 537 578
- 538 579
- 539 [59] S. Ronski and G. Budéus, Time series of winter convection in the Greenland Sea, *J. Geophys. Res.* **110** (2005). 580
- 540 581
- 541 [60] J. K. Rieck, C. W. Böning, and K. Getzlaff, The nature of eddy kinetic energy in the Labrador Sea: Different types of mesoscale eddies, their temporal variability, and impact on deep convection, *J. Phys. Oceanogr.* **49**, 2075 (2019). 582
- 542 583
- 543 584
- 544 585
- 545 [61] D. B. Chelton, M. G. Schlax, and R. M. Samelson, Global observations of nonlinear mesoscale eddies, *Progr. Oceanogr.* **91**, 167 (2011). 586
- 546 587
- 547 588
- 548 589
- 549 590
- 550 591
- 551 [62] P. Gaube, D. J. McGillicuddy Jr, and A. J. Moulin, Mesoscale eddies modulate mixed layer depth globally, *Geophys. Res. Lett.* **46**, 1505 (2019). 592
- 552 593
- 553 594
- 554 595
- 555 [63] J. Chanut, B. Barnier, W. Large, L. Debreu, T. Penduff, J. M. Molines, and P. Mathiot, Mesoscale eddies in the Labrador Sea and their contribution to convection and restratification, *J. Phys. Oceanogr.* **38**, 1617 (2008). 596
- 556 597
- 557 598
- 558 599
- 559 600
- 560 [64] N. Wunderling, R. Winkelmann, J. Rockström, S. Loriani, D. I. Armstrong McKay, P. D. Ritchie, B. Sakschewski, and J. F. Donges, Global warming overshoots increase risks of climate tipping cascades in a network model, *Nat. Clim. Change* **13**, 75 (2023). 601
- 561 602
- 562 603
- 563 604
- 564 [65] C. Danek, P. Scholz, and G. Lohmann, Effects of high resolution and spinup time on modeled North Atlantic circulation, *J. Phys. Oceanogr.* **49**, 1159 (2019). 605
- 565 606
- 566 607
- 567 608
- 568 [66] L. G. Henry, J. F. McManus, W. B. Curry, N. L. Roberts, A. M. Piotrowski, and L. D. Keigwin, North Atlantic Ocean circulation and abrupt climate change during the last glaciation, *Science* **353**, 470 (2016). 609
- 569 610
- 570 611
- 571 612
- 572 [67] S. Manabe and R. T. Wetherald, The effects of doubling the CO<sub>2</sub> concentration on the climate of a general circulation model, *J. Atmos. Sci.* **32**, 3 (1975). 613
- 573 614
- 574 615
- 575 [68] K. Hasselmann, Stochastic climate models part I. Theory, *Tellus* **28**, 473 (1976). 616
- 576 617
- 577 618
- 578 [69] K. Hasselmann, Optimal fingerprints for the detection of time-dependent climate change, *J. Clim.* **6**, 1957 (1993). 619
- 579 620
- 580 621
- 581 [70] F. Colleoni, L. De Santis, C. S. Siddoway, A. Bergamasco, N. R. Golledge, G. Lohmann, S. Passchier, and M. J. Siebert, Spatio-temporal variability of processes across antarctic ice-bed-ocean interfaces, *Nat. Commun.* **9**, 1 (2018). 622
- 582 623
- 583 624
- 584 625
- 585 [71] P. M. Ruti *et al.*, Med-cortex initiative for mediterranean climate studies, *Bull. Am. Meteorol. Soc.* **97**, 1187 (2016). 626
- 586 627
- 587 628
- 588 [72] D. A. Smeed, G. D. McCarthy, S. A. Cunningham, E. Frajka-Williams, D. Rayner, W. Johns, C. S. Meinen, M. O. Baringer, B. I. Moat, A. Duchez *et al.*, Observed decline of the Atlantic meridional overturning circulation 2004–2012, *Ocean Sci.* **10**, 29 (2014). 629
- 589 630
- 590 631
- 591 [73] M. Srokosz and H. Bryden, Observing the Atlantic meridional overturning circulation yields a decade of inevitable surprises, *Science* **348** (2015). 632
- 592 633
- 593 634
- 594 635
- 595 636
- 596 637
- 597 638
- 598 639
- 599 640
- 600 641
- 601 642
- 602 643
- 603 644
- 604 645
- 605 646
- 606 647
- 607 648
- 608 649
- 609 650
- 610 651
- 611 652
- 612 653
- 613 654
- 614 655
- 615 656
- 616 657
- 617 658
- 618 659
- 619 660
- 620 661
- 621 662
- 622 663
- 623 664
- 624 665
- 625 666
- 626 667
- 627 668
- 628 669
- 629 670
- 630 671
- 631 672
- 632 673
- 633 674
- 634 675
- 635 676
- 636 677
- 637 678
- 638 679
- 639 680
- 640 681
- 641 682
- 642 683
- 643 684
- 644 685
- 645 686
- 646 687
- 647 688
- 648 689
- 649 690
- 650 691
- 651 692
- 652 693
- 653 694
- 654 695
- 655 696
- 656 697
- 657 698
- 658 699
- 659 700
- 660 701
- 661 702
- 662 703
- 663 704
- 664 705
- 665 706
- 666 707
- 667 708
- 668 709
- 669 710
- 670 711
- 671 712
- 672 713
- 673 714
- 674 715
- 675 716
- 676 717
- 677 718
- 678 719
- 679 720
- 680 721
- 681 722
- 682 723
- 683 724
- 684 725
- 685 726
- 686 727
- 687 728
- 688 729
- 689 730
- 690 731
- 691 732
- 692 733
- 693 734
- 694 735
- 695 736
- 696 737
- 697 738
- 698 739
- 699 740
- 700 741
- 701 742
- 702 743
- 703 744
- 704 745
- 705 746
- 706 747
- 707 748
- 708 749
- 709 750
- 710 751
- 711 752
- 712 753
- 713 754
- 714 755
- 715 756
- 716 757
- 717 758
- 718 759
- 719 760
- 720 761
- 721 762
- 722 763
- 723 764
- 724 765
- 725 766
- 726 767
- 727 768
- 728 769
- 729 770
- 730 771
- 731 772
- 732 773
- 733 774
- 734 775
- 735 776
- 736 777
- 737 778
- 738 779
- 739 780
- 740 781
- 741 782
- 742 783
- 743 784
- 744 785
- 745 786
- 746 787
- 747 788
- 748 789
- 749 790
- 750 791
- 751 792
- 752 793
- 753 794
- 754 795
- 755 796
- 756 797
- 757 798
- 758 799
- 759 800
- 760 801
- 761 802
- 762 803
- 763 804
- 764 805
- 765 806
- 766 807
- 767 808
- 768 809
- 769 810
- 770 811
- 771 812
- 772 813
- 773 814
- 774 815
- 775 816
- 776 817
- 777 818
- 778 819
- 779 820
- 780 821
- 781 822
- 782 823
- 783 824
- 784 825
- 785 826
- 786 827
- 787 828
- 788 829
- 789 830
- 790 831
- 791 832
- 792 833
- 793 834
- 794 835
- 795 836
- 796 837
- 797 838
- 798 839
- 799 840
- 800 841
- 801 842
- 802 843
- 803 844
- 804 845
- 805 846
- 806 847
- 807 848
- 808 849
- 809 850
- 810 851
- 811 852
- 812 853
- 813 854
- 814 855
- 815 856
- 816 857
- 817 858
- 818 859
- 819 860
- 820 861
- 821 862
- 822 863
- 823 864
- 824 865
- 825 866
- 826 867
- 827 868
- 828 869
- 829 870
- 830 871
- 831 872
- 832 873
- 833 874
- 834 875
- 835 876
- 836 877
- 837 878
- 838 879
- 839 880
- 840 881
- 841 882
- 842 883
- 843 884
- 844 885
- 845 886
- 846 887
- 847 888
- 848 889
- 849 890
- 850 891
- 851 892
- 852 893
- 853 894
- 854 895
- 855 896
- 856 897
- 857 898
- 858 899
- 859 900
- 860 901
- 861 902
- 862 903
- 863 904
- 864 905
- 865 906
- 866 907
- 867 908
- 868 909
- 869 910
- 870 911
- 871 912
- 872 913
- 873 914
- 874 915
- 875 916
- 876 917
- 877 918
- 878 919
- 879 920
- 880 921
- 881 922
- 882 923
- 883 924
- 884 925
- 885 926
- 886 927
- 887 928
- 888 929
- 889 930
- 890 931
- 891 932
- 892 933
- 893 934
- 894 935
- 895 936
- 896 937
- 897 938
- 898 939
- 899 940
- 900 941
- 901 942
- 902 943
- 903 944
- 904 945
- 905 946
- 906 947
- 907 948
- 908 949
- 909 950
- 910 951
- 911 952
- 912 953
- 913 954
- 914 955
- 915 956
- 916 957
- 917 958
- 918 959
- 919 960
- 920 961
- 921 962
- 922 963
- 923 964
- 924 965
- 925 966
- 926 967
- 927 968
- 928 969
- 929 970
- 930 971
- 931 972
- 932 973
- 933 974
- 934 975
- 935 976
- 936 977
- 937 978
- 938 979
- 939 980
- 940 981
- 941 982
- 942 983
- 943 984
- 944 985
- 945 986
- 946 987
- 947 988
- 948 989
- 949 990
- 950 991
- 951 992
- 952 993
- 953 994
- 954 995
- 955 996
- 956 997
- 957 998
- 958 999
- 959 1000
- 960 1001
- 961 1002
- 962 1003
- 963 1004
- 964 1005
- 965 1006
- 966 1007
- 967 1008
- 968 1009
- 969 1010
- 970 1011
- 971 1012
- 972 1013
- 973 1014
- 974 1015
- 975 1016
- 976 1017
- 977 1018
- 978 1019
- 979 1020
- 980 1021
- 981 1022
- 982 1023
- 983 1024
- 984 1025
- 985 1026
- 986 1027
- 987 1028
- 988 1029
- 989 1030
- 990 1031
- 991 1032
- 992 1033
- 993 1034
- 994 1035
- 995 1036
- 996 1037
- 997 1038
- 998 1039
- 999 1040
- 1000 1041